

MALAYSIAN JOURNAL OF ANALYTICAL SCIENCES

Published by The Malaysian Analytical Sciences Society

ISSN 1394 - 2506

PHOTOCATALYTIC DEGRADATION OF METHYLENE BLUE WITH SILVER DOPED ZNO NANOPARTICLES GROWN ON MICROSCOPIC SAND PARTICLES

(Degradasi Metilena Biru Menggunakan Nanopartikel ZnO Sebagai Fotomangkin yang Didopkan dengan Perak Tumbuh di atas Pasir Bersaiz Mikro)

Nur Azmina Mohamed Safian¹*, Roslan Md Nor¹, Hartini Ahmad Rafaie², Siti Fairus Abdul Sani¹, Zurina Osman¹

¹Department of Physics, Faculty of Sciences, University of Malaya, 50603 Kuala Lumpur, Malaysia ²Unit of Physics, School of Science, Universiti Teknologi MARA Pahang, Jengka, 26400 Bandar Tun Abdul Razak, Jengka Pahang, Malaysia

*Corresponding author: nurazminasafian@siswa.um.edu.my

Received: 4 December 2016; Accepted: 1 December 2017

Abstract

Pure and Ag doped ZnO nanoparticles were synthesized on microscopic sand particles by sol-gel method. Silver nitrate was used as the doping precursor, Ag doping levels of 1.3 to 7.7 of Ag/Zn ratios were obtained based on energy dispersive X-ray spectroscopy analysis. X-ray diffraction results show that a ZnO (101) peak of Ag doped samples are shifted towards lower degree which around 0.17° compared to pure ZnO NPs, indicating the existence of doping in the Ag doped samples. The pure and Ag doped ZnO samples were used as photocatalysts in the degradation of methylene blue under UV irradiation. Photodegradation efficiency based on the pseudo-first kinetics model gave measured values of the photodegradation rate, k of 8.9, 11.8, 12.7, 14.8 and 17.4 x 10⁻³ min⁻¹ for pure, 1.3, 1.6, 1.7 and 2.4 of Ag/Zn ratios, respectively. At higher doping levels of 3.3 and 7.7 of Ag/Zn ratios, the k values receded to 12.7 and 12.0 x 10⁻³ min⁻¹, respectively. The increasing trend on k values can be due to the doping defect levels which trapped the recombining electrons, thus lengthening the lifetime of the electron hole pairs.

Keywords: photocatalysis, Ag doped ZnO, nanoparticles

Abstrak

Nanopartikel ZnO tulen dan nanopartikel ZnO yang didopkan dengan perak (Ag) telah disintesiskan di atas pasir bersaiz mikro menggunakan kaedah sol-gel. Argentum nitrat digunakan sebagai sumber Ag, dapatan tahap pendopan adalah 1.3 sehingga 7.7 nisbah Ag kepada Zn (Ag/Zn). Berdasarkan keputusan spektroskopi sinar-X, terdapat peralihan kedudukan puncak ZnO (101) sebanyak 0.17° jika dibandingkan antara ZnO tulen dan sampel ZnO yang didopkan dengan Ag. Ini menunjukkan berlaku pendopan di dalam sampel nanopartikel ZnO yang didopkan dengan Ag. Semua sampel diuji sebagai fotomangkin di dalam degradasi metilena biru di bawah sinar UV. Kecekapan degradasi dikira menggunakan model kinetik pseudo-pertama dan memberikan nilai kadar degradasi, k iaitu masing-masing 8.9, 11.8, 12.7, 14.8 dan 17.4 x 10⁻³ min⁻¹ untuk sampel ZnO tulen, 1.3, 1.6, 1.7 dan 2.4 untuk nisbah Ag/Zn. Pada tahap pendopan yang tinggi iaitu 3.3 dan 7.7 Ag/Zn, nilai k berkurangan kepada 12.7 dan 12.0 x 10⁻³ min⁻¹. Peningkatan nilai k adalah disebabkan oleh kesan pendopan di mana elektron terperangkap untuk pergabungan semula dan memangjangkan jangka hayat pasangan elektron dan lubang.

Kata kunci: fotomangkin, perak didopkan ZnO, nanopartikel

Introduction

Since 1972, the capability of ZnO in the degradation of wastewater has been studied [1]. Due to its remarkable features which has wide band gap (3.37 eV) at room temperature and high exciton binding energy of approximately 60 meV has made ZnO as a perfect candidate in photocatalyst application. To achieve high photocatalytic degradation efficiency of wastewater, ZnO photocatalyst must offer large specific surface area and a high efficiency for segregation photogenerated electron and holes. The most efficient way to accelerate the charge carrier separation by dope with noble metals. Silver (Ag) has been reported as the best element to dope with ZnO due to its high solubility [2] and can act as a sink to collect photogenerated electrons from the conduction band of ZnO [3]. Furthermore, Ag 4d and oxygen 2p states were overlapped to form impurity band. This lead to the Fermi level shifted toward valence band and induced properties in ZnO [4].

Although there have many reports on the properties and photocatalysis efficiency of Ag doped ZnO, there is still lack of understanding in details about photodegradation mechanism using Ag doped ZnO. In this work, the differences of the photocatalytic degradation between ZnO and Ag doped ZnO on microscopic sand has been studied. Also, the effect of Ag ions on the morphology, defect and photocatalytic efficiency of all samples were investigated in detailed.

Materials and Methods

Synthesis of Ag doped ZnO Nanoparticles on microscopic sand

ZnO NPs growth on microscopic sand by simple seeded solution process using zinc acetate, Zn(O₂CCH₃)₂ which was prepared in absolute ethanol at 0.0005 mol concentration. The sand were soaked for 5 minutes and then dry at 300 °C for 10 minutes. The process were repeated for three times before calcination process. Zinc nitrate hexahydrate (Zn(NO₃)₂·6H₂O) and hexamethylenetetramine (HMTA) were initially combined at the molar ratio of 1:1 in deionized water for growth solution. Then, silver nitrate hexahydrate (AgNO₃) were added in mixture solution at 1.0 to 3.5 mol % with 0.5 mol % increment. 5g of the seeded sand were added in the doping solution and stirred continuously at 100 °C for 6 hours. After completing the growth process, the Ag doped ZnO NPs grown on sand were wash and rinsed several times thoroughly in DI water and calcined at 300 °C for 2 hours.

Characterization of Ag doped ZnO Nanoparticles

The as-prepared Ag doped ZnO NPs grown on sand were examined by several characterization techniques. The elemental of as-prepared nanomaterials were characterized by energy dispersive spectroscopy (EDX - JSM 7600-F). The morphologies were examined by field emission scanning electron microscopy (FESEM – JSM 7600-F). The crystallinity and optical properties of ZnO NPs samples were studied by X-ray diffractometer (XRD - EMPYREAN, PANalytical) and photoluminescence (PL-In-Via Raman Microscope) spectroscopy, respectively.

Photocatalytic degradation of methylene blue using Ag doped ZnO nanoparticles

The photocatalytic performances of the samples were evaluated by the decomposition of 0.5 mg/ 100 ml methylene blue solution under UV light at 254 nm wavelength. An amount 1g of samples were added in the MB solution and placed in the dark mood for 30 minutes before switching the UV lamp (6 Watt, UVGL-58). Afterwards, absorption spectra of the MB solutions were taken and analyzed by ultraviolet-visible (UV-Vis - EVOLUTION 201, Thermo Scientific) spectroscopy.

Results and Discussion

The present of Ag element in the ZnO samples grown on microscopic sand were evidenced by EDX spectra as shown in Figure 1. The amount of Ag doped ZnO were calculated by atomic percent (at. %) which leads to 1.3, 1.6, 1.7, 2.4, 3.3 and 7.7 of Ag/Zn ratios for 1.0, 1.5, 2.0, 2.5, 3.0 and 3.5 mol %, respectively as tabulated in Table 1. As the amount of Ag doped increases, a strong peak of $Ag_{L\alpha}$ and $Ag_{L\beta}$ appeared in ZnO samples at 2.97 and 2.98 KeV especially for ZnO 3.3 and 7.7 of Ag/Zn ratio samples.

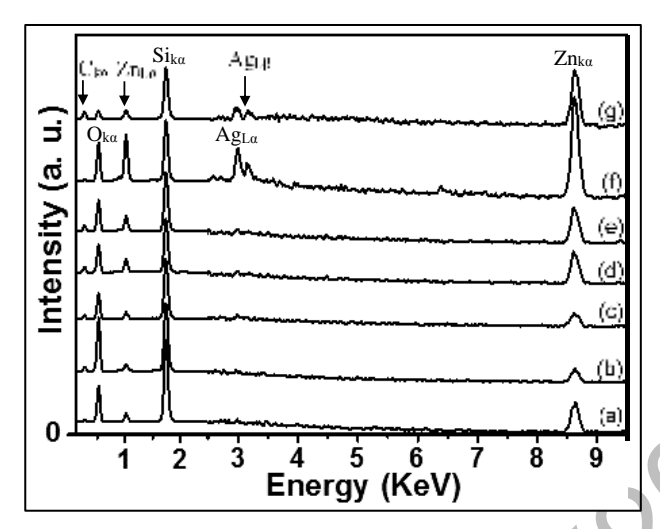


Figure 1. EDX spectra of (a) pure ZnO NPs and Ag doped ZnO NPs grown on microscopic sand at (b) 1.0, (c) 1.5, (d) 2.0, (e) 2.5, (f) 3.0 and (g) 3.5 mol% of AgNO₃

Table 1. The summary of elements composition of pure and Ag doped ZnO NPs grown on microscopic sand based on EDX analysis

(Samples)		At. % Ag Zn O Si				[Ag]/[Zn] x 100
(a)	pure ZnO NPs	-	7.13	36.39	43.54	0
(b)	1.0 mol% AgNO ₃	59.54	16.90	1.55	0.02	1.3
(c)	1.5 mol% AgNO ₃	45.22	16.65	3.72	0.06	1.6
(d)	2.0 mol% AgNO ₃	54.53	24.85	7.05	0.12	1.7
(e)	2.5 mol% AgNO ₃	48.48	21.03	2.09	0.05	(2.4)
(f)	3.0 mol% AgNO ₃	53.92	21.68	11.84	0.39	(3.3)
(g)	3.5 mol % AgNO ₃	22.90	18.93	2.60	0.20	(7.7)

The images of surface morphology, particles sizes and shape of the ZnO and Ag doped ZnO NPs grown on sand were obtained by FESEM as shown in Figure 2. High density of the ZnO and Ag doped ZnO NPs were observed throughout the sand surface with the sizes of particles in the range of tens to hundreds of nanometers. From the observation, most of the particles in the ZnO and Ag doped ZnO NPs samples were exhibited spindles-like shape which has wide in the middle and tapers at both ends. The particles sizes were found to be mixed between small and large particles in the 2.4 of Ag/Zn ratio sample as shown in Figure 2(e). These small particles might increase the surface area of Ag doped ZnO samples which will enhance its light absorption and improve its photocatalytic activity. The images also show that the particles sizes of Ag doped ZnO seem like become bigger at high Ag content. The changes in particles sizes was believed due to the aggregation of Ag and Zn particle into bigger cluster. This can cause decreased light utilization rate and led to low photocatalytic activity. The biggest particles diameters were measured in the Ag doped ZnO at 7.7 of Ag/Zn ratio which around 223 to 225 nm.

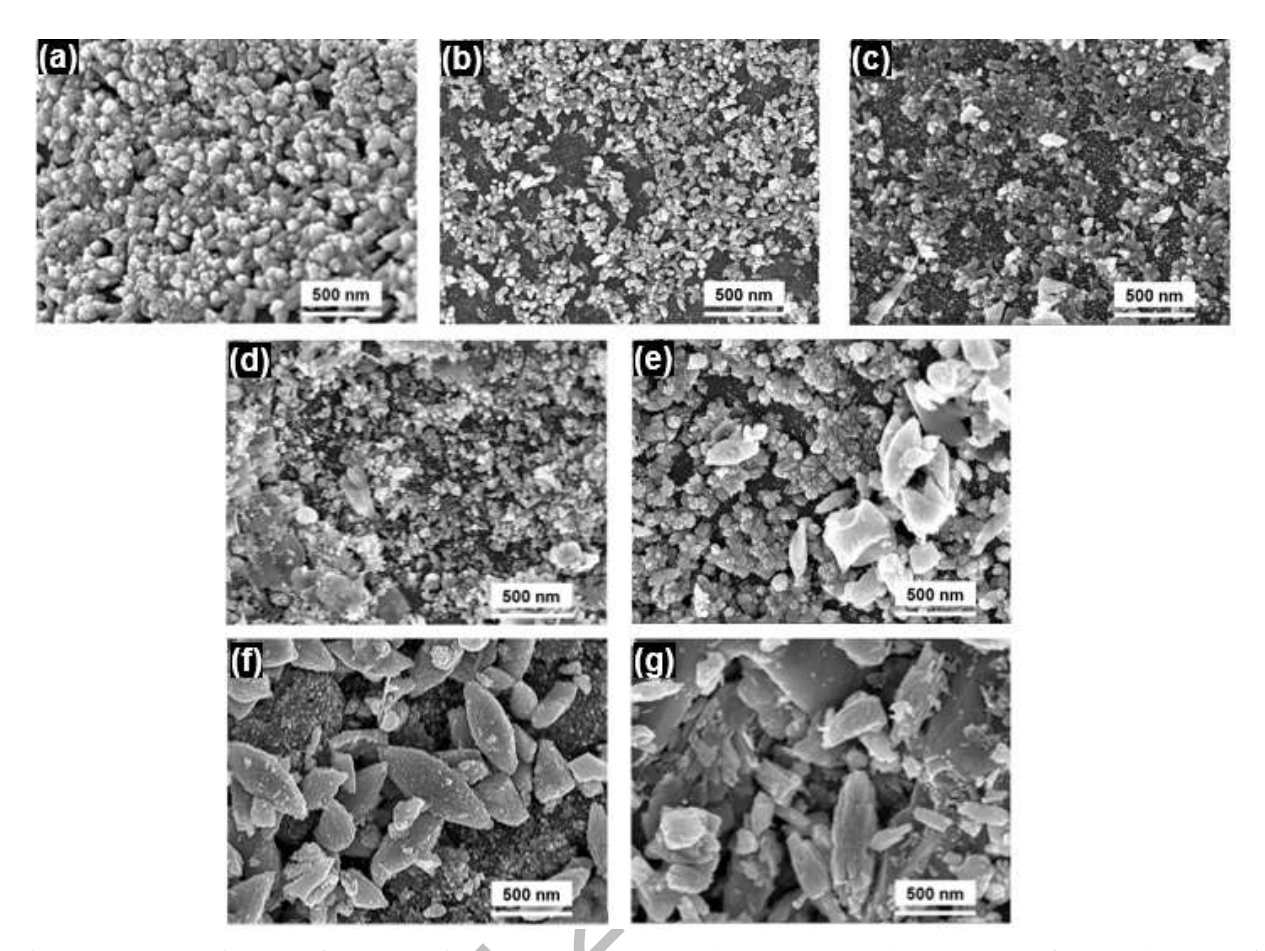


Figure 2. FESEM images of as-synthesized (a) pure ZnO NPs, (b) 1.3, (c) 1.6, (d) 1.7, (e) 2.4, (f) 3.3 and (g) 7.7 of Ag/Zn ratios

The typical XRD patterns of pure ZnO nanoparticles and Ag doped ZnO grown on sand are illustrated in Figure 3(a). Clearly, all samples showed common ZnO peaks at 31.8°, 34.4°, 36.3°, 47.6°, 56.7°, 62.9°, 66.4° and 69.2°. The peaks position can be indexed to the wurtzite crystal ZnO structure (JCPDS File No. 01-79-2205) and correspond to (100), (002), (101), (102), (110), (103), (200) and (201), respectively. The others peaks at 39.7°, 40.4°, 42.6°, 45.9°, 50.4°, 55.1° and 60.1° can be indexed to the (012), (111), (200), (201), (134), (022) and (211) reflection planes of quartz based on the JCPDS file no. 46-1045. Figure 3(b) shows an enlarged view of XRD patterns of ZnO and Ag doped ZnO grown on microscopic sand. Noting that the peak position of (101) reflection peak had shifted toward lower values as the Ag dopant increases. The shift might be due to the partial substitution of Ag⁺ in the ZnO lattice and causes the increases of lattice constant a and c [5, 6]. This occurred probably related to the differentiation of ionic radii between Ag⁺ and Zn²⁺ ions which 1.22 Å and 0.74 Å, respectively.

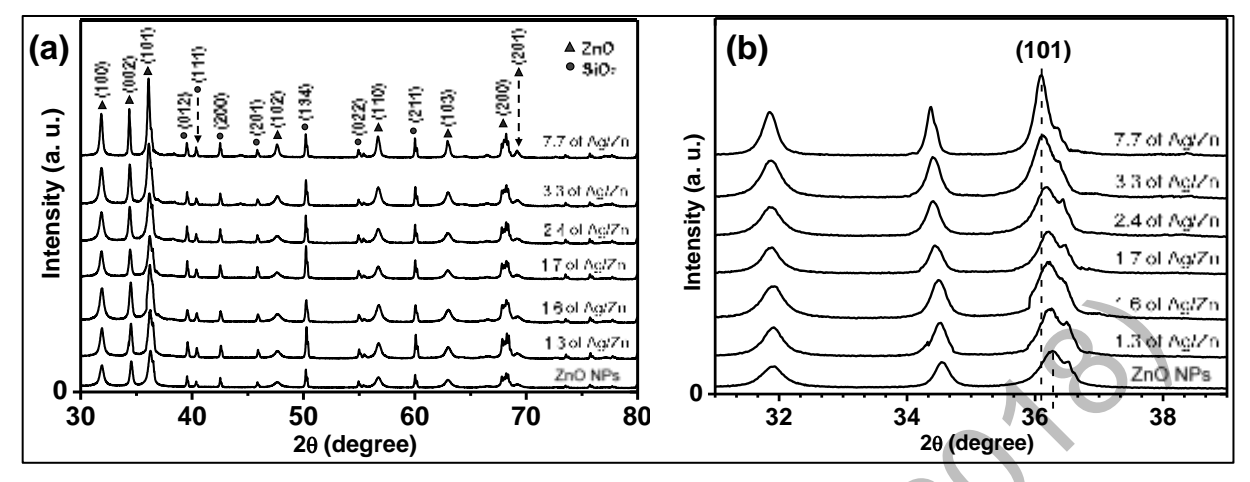


Figure 3. (a) Full range of XRD patterns and (b) shift detail of ZnO (101) peak of ZnO and Ag doped ZnO grown on sand

Figure 4 shows the photoluminescence spectra of pure and Ag doped ZnO sample in the range of 200 to 900 nm. There are two peaks showed in PL spectra which the obvious and broad peak was appeared at 500 to 800 nm and small peak was appeared at round 350 to 420 nm as shown in inset graph in Figure 4. The small peaks below 420 nm were indicated as near-band-edge (NBE) emission which associated with exciton emission which obtained in ZnO and 2.4 of Ag/Zn ratio sample. The NBE emission usually caused by band structural deformation resulting from lattice deformation [7]. This peak which are attributed to the reduction of oxygen interstitials at ZnO surface [8]. By reducing the defect of oxygen interstitials, it might enhanced the photocatalytic activity of ZnO as photocatalyst. The center of these peaks position were obtained at 394 nm for ZnO NPs and 404 nm for 2.4 of Ag/Zn ratio sample.

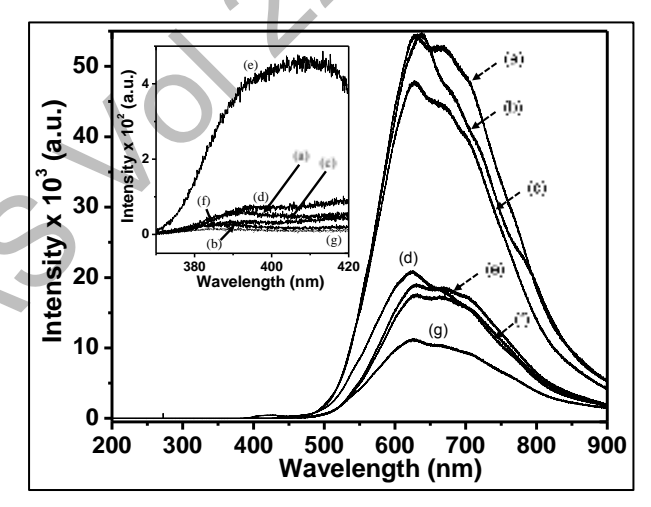


Figure 4. Full range PL spectra from 300 to 900 nm. The inset graph shows enlargement PL spectra at range 370 to 490 nm of (a) pure ZnO NPs, (b) 1.3, (c) 1.6, (d) 1.7, (e) 2.4, (f) 3.3 and (g) 7.7 of Ag/Zn ratios

The broad peak at range 500 to 800 nm in the PL spectra was called as deep level emission. The deep level emission is usually related to the structural defect and impurities of samples [7]. Figure 5 (a) to (g) show the deep level emission for pure ZnO NPs, 1.3, 1.6, 1.7, 2.4, 3.3 and 7.7 of Ag/Zn ratio samples, respectively. The fitting of broad spectrum was done using Gaussian distribution which shows four major peaks around 553 to 567 nm, 608 to 614 nm, 653 to 684 and 713 to 780 nm. The peak around 553 to 567 nm was believed attributed to the transition of zinc

interstitial to zinc vacancies. While two peaks at range 608-614nm and 653-674 nm were known as orange-yellow and orange-red emission respectively, obtained due to the structural defect and single ionized vacancy [9, 10] as well as oxygen interstitial [11]. The single negatively charged interstitial oxygen ion inside the lattice occurs due to the loss of oxygen ions within the crystal lattice [12]. The last peak around 713 to 780 nm was appeared which corresponding to the oxygen vacancies and zinc interstitials [13].

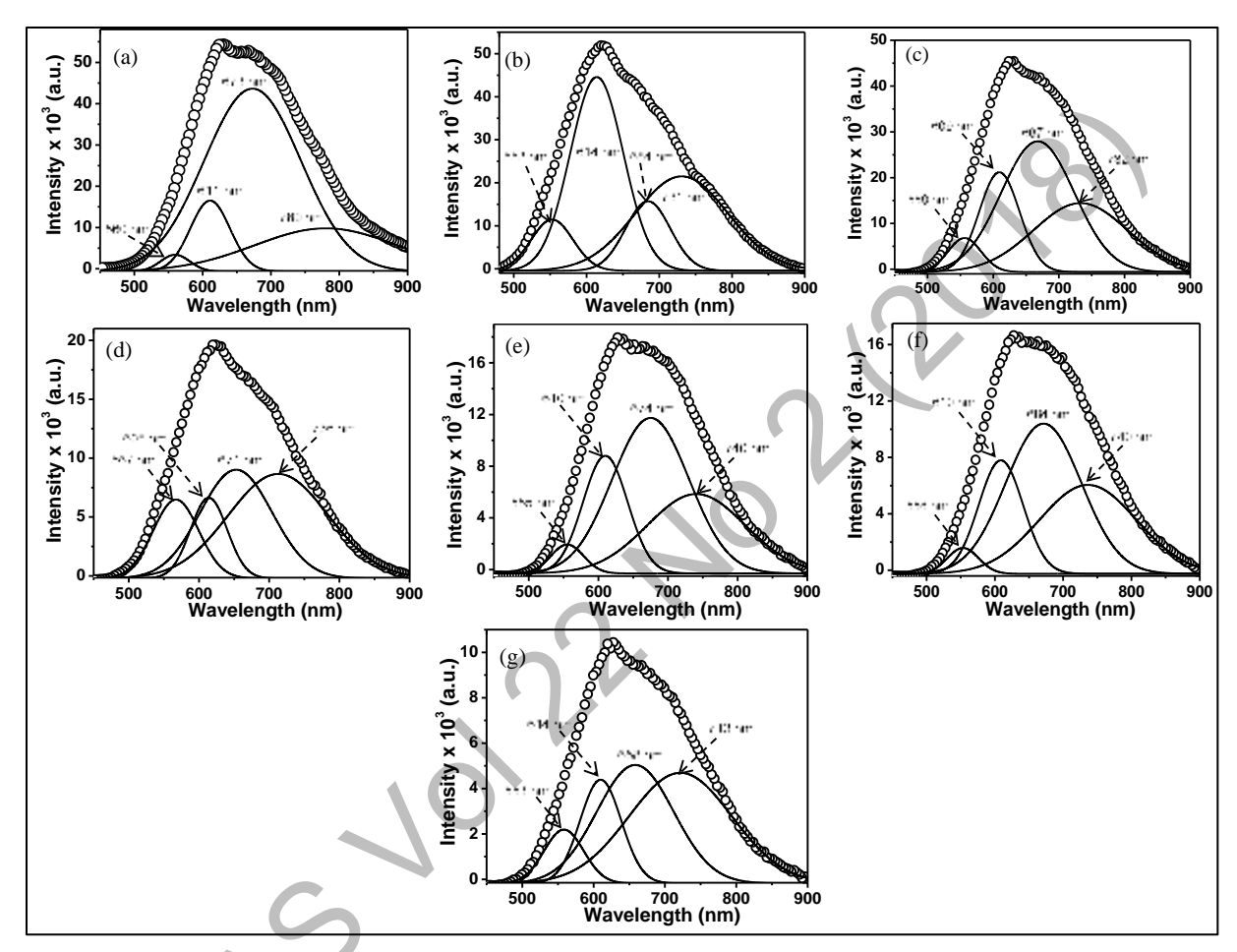


Figure 5. Gaussian fitted PL spectrum of (a) pure ZnO NPs, (b) 1.3 (c) 1.6, (d) 1.7, (e) 2.4, (f) 3.3 and (g) 7.7 of Ag/Zn ratios

The absorption spectra of photodegradation 100 ml MB solution using (a) pure ZnO and Ag doped ZnO at (b) 1.3, (c) 1.6, (d) 1.7, (e) 2.4, (f) 3.3 and (g) 7.7 of Ag/Zn ratios under UV light irradiation for 150 mins are shown in Figure 6. The UV-vis spectra was seen to be similar for all samples which is the tremendous peak of MB dye was appeared at 664 nm. The intensity of peak at 664 nm were gradually decreased with each 15 minutes increment irradiation time. The curve of absorption for 2.4 of Ag/Zn ratio of Ag doped ZnO photocatalyst at 150 minutes irradiation time was shows nearly horizontal meaning the MB solution was almost completely degrade.

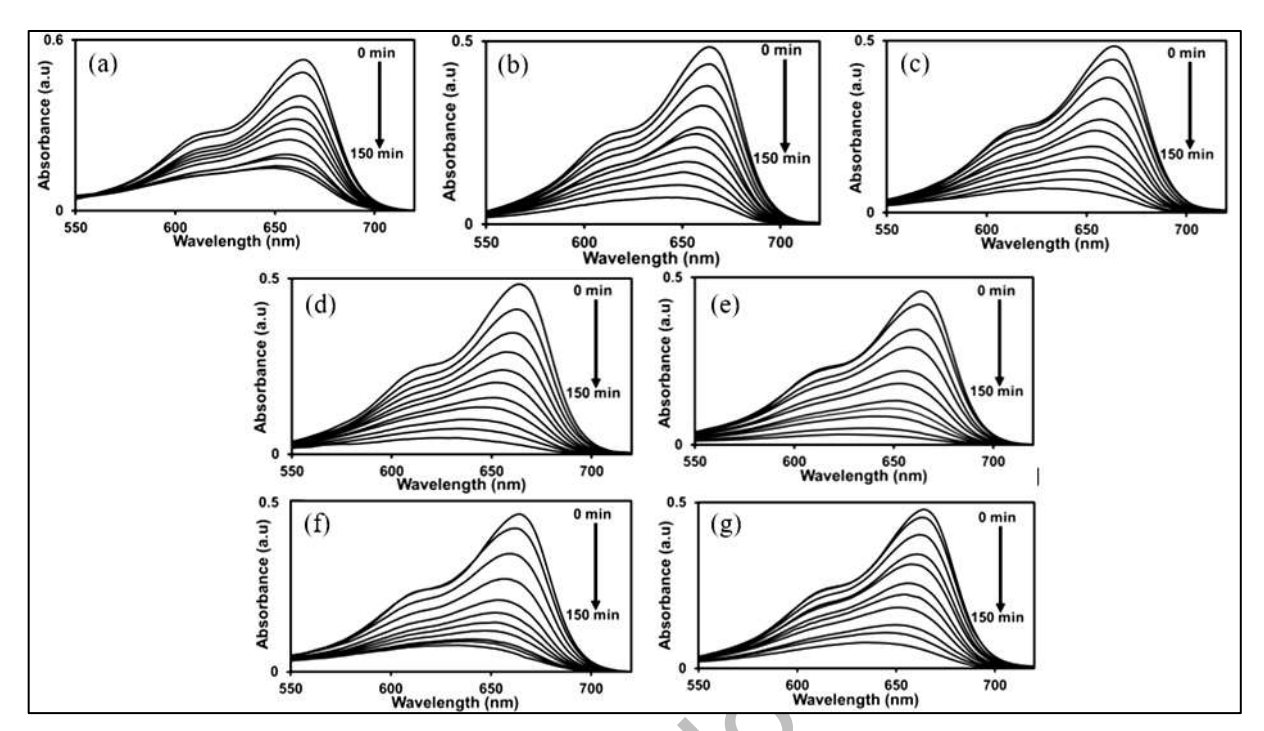


Figure 6. UV-vis absorption spectra of photodegradation 100 ml of 5 mg/l MB solution under UV lamp irradiation using: (a) pure ZnO NPs, (b) 1.3 (c) 1.6, (d) 1.7, (e) 2.4, (f) 3.3 and (g) 7.7 of Ag/Zn ratios as photocatalysts

Figure 7(a) shows the photodegradation efficiency (%) for 150 minutes irradiation time for all samples. The highest photodegradation efficiency was calculated at 2.4 of Ag/Zn ratio sample which was 93.3%. Then followed by 1.7, 1.6, 1.3, 7.7 and 3.3 of Ag/Zn ratio samples which were 90.4%, 85.3%. 84.8%, 83.6% and 83.1%, respectively. The lowest photodegradation efficiency was obtained from pure ZnO sample which around 71.7%. Based on results, it clearly demonstrated that ZnO doped with Ag degrades dye more efficiently than pure ZnO. It is evident that doping of ZnO with transition metals like Ag enhances photocatalytic activities of ZnO. However, further increasing the Ag content in the ZnO samples show decreases of photocatalytic activity as obtained at 3.3 and 7.7 of Ag/Zn ratio samples. It was believed due to the existence of bulk defects which the only ones have bad effects on the photocatalytic activity [14]. The agglomeration of small particles into bigger clusters has formed impurities or bulk defect as confirmed by FESEM analysis. Consequently, decreased the surface area of photocatalyst and decelerates the oxidation and reduction process of MB solution.

The photodegradation rate constant, k of pure ZnO and Ag doped ZnO NPs samples were obtained by plotting ln (C/C_o) against irradiation time as shown in Figure 7(b). The linear plots revealed that the photodegradation of MB has follow pseudo-first order reaction kinetics. The lowest value of k was calculated at pure ZnO NPs sample which $8.9 \times 10^{-3} \text{ min}^{-1}$ then as dopant increase from 1.3 to 2.4 of Ag/Zn ratio, the value of k has been increased from 11.8 to $17.4 \times 10^{-3} \text{ min}^{-1}$ as shown in Figure 7(c). The value of k then decreases as increase the Ag content in ZnO sample which around 12.7 to 12.0 x 10^{-3} min^{-1} at 3.3 and 7.7 of Ag/Zn ratio sample, respectively. At the optimum Ag content which was 2.4 of Ag/Zn ratio, the Ag particles that deposited with the ZnO can act as electron-hole separation center. The electron might be transfer from the ZnO conduction band to metallic silver particles at interface. In contrast, high Ag dopant is detrimental to the photodegradation efficiency which the Ag particles can act as electron hole recombination center, thereby decreasing the photocatalytic activity of ZnO.

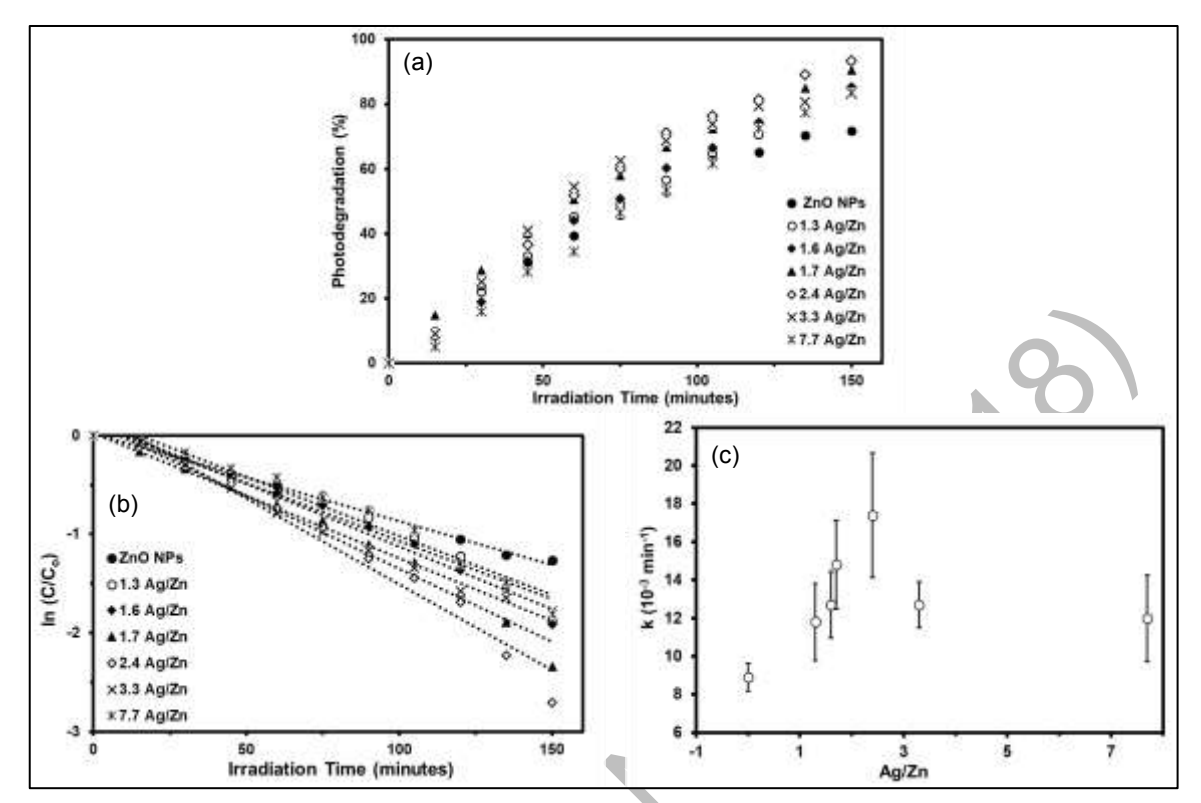


Figure 7. (a) The percentage of photodegradation MB solution for 150 minutes. (b) Linear plots of ln (C/C_o) for the photodegradation of MB in the presence of sand-ZnO and Ag doped ZnO samples and (c) the changes of k values as a function of Ag content.

Conclusion

Ag doped ZnO with varied Ag content from 1.3 to 7.7 of Ag/Zn ratios has been successfully synthesized on the microscopic sand. The EDX has shown the existence of Ag element in the samples and the shifted ZnO [101] peak of XRD has proven that the Ag particles has been doped in the ZnO samples. The FESEM images show that the diameters and structures of ZnO were slightly change to bigger sizes as increases of Ag dopant. The defects introduce additional states in the band gap of ZnO which act as electron trapping centers and contributed in the prolonging a lifetime of charge carriers. The photocatalytic activity for Ag doped ZnO at 2.4 of Ag/Zn ratio has increase was almost twice compared to the pure ZnO which from 8.9 to 17.4 x 10⁻³ min⁻¹. Therefore, the Ag doped ZnO samples grown on sand had shown very interesting characteristics and promising as good photocatalytic agent as well as has good potential for application on the water purification especially in industrial sector.

Acknowledgement

The authors are grateful to the Institute of Research Management and Monitoring, University of Malaya for providing a postgraduate research grant (Project Code: PG110-2015A) and Department of Physics, University of Malaya for financial and facilities support of this work.

References

- 1. Tanaka, K. and Blyholder, G. (1972). Photocatalytic reactions on zinc oxide. III. Hydrogenation of ethylene. *The Journal of Physical Chemistry*, 76(10): 1394-1397.
- 2. Yan, Y., Al-Jassim, M. M. and Wei, S. H. (2006). Doping of ZnO by Group-IB elements. *Applied physics letters*, 89(18): 181912.
- 3. Ren, C., Yang, B., Wu, M., Xu, J., Fu, Z., Guo, T., Zhao, Y. and Zhu, C. (2010). Synthesis of Ag/ZnO nanorods array with enhanced photocatalytic performance. *Journal of Hazardous materials*, 182(1): 123-129.

- 4. Hosseini, S. M., Sarsari, I. A., Kameli, P. and Salamati, H. (2015). Effect of Ag doping on structural, optical, and photocatalytic properties of ZnO nanoparticles. *Journal of Alloys and Compounds*, 640: 408-415.
- 5. Karunakaran, C., Rajeswari, V. and Gomathisankar, P. (2011). Combustion synthesis of ZnO and Ag-doped ZnO and their bactericidal and photocatalytic activities. *Superlattices and Microstructures*, 50(3): 234-241.
- 6. Amornpitoksuk, P., Suwanboon, S., Sangkanu, S., Sukhoom, A., Muensit, N. and Baltrusaitis, J. (2012). Synthesis, characterization, photocatalytic and antibacterial activities of Ag-doped ZnO powders modified with a diblock copolymer. *Powder Technology*, 219: 158-164.
- 7. Tamargo, M. C. (2002). II-VI semiconductor materials and their applications (Vol. 12). CRC Press.
- 8. Sun, W. C., Yeh, Y. C., Ko, C. T., He, J. H. and Chen, M. J. (2011). Improved characteristics of near-band-edge and deep-level emissions from ZnO nanorod arrays by atomic-layer-deposited Al₂O₃ and ZnO shell layers. *Nanoscale Research Letters*, 6(1): 556.
- 9. Vanheusden, K., Warren, W. L., Seager, C. H., Tallant, D. R., Voigt, J. A. and Gnade, B. E. (1996). Mechanisms behind green photoluminescence in ZnO phosphor powders. *Journal of Applied Physics*, 79 (10): 7983-7990.
- 10. Wu, J. J. and Liu, S. C. (2002). Low-temperature growth of well-aligned ZnO nanorods by chemical vapor deposition. *Advanced Materials*, 14(3): 215-218.
- 11. Liu, M., Kitai, A. H. and Mascher, P. (1992). Point defects and luminescence centres in zinc oxide and zinc oxide doped with manganese. *Journal of Luminescence*, 54(1): 35-42.
- 12. Wu, X. L., Siu, G. G., Fu, C. L. and Ong, H. C. (2001). Photoluminescence and cathodoluminescence studies of stoichiometric and oxygen-deficient ZnO films. *Applied Physics Letters*, 78(16): 2285-2287.
- 13. Djurišić, A. B., Leung, Y. H., Tam, K. H., Hsu, Y. F., Ding, L., Ge, W. K., Zhong, Y. C., Wong, K. S., Chan, W. K., Tam, H. L. and Cheah, K. W. (2007). Defect emissions in ZnO nanostructures. *Nanotechnology*, 18(9): 095702.
- 14. Kong, M., Li, Y., Chen, X., Tian, T., Fang, P., Zheng, F. and Zhao, X. (2011). Tuning the relative concentration ratio of bulk defects to surface defects in TiO₂ nanocrystals leads to high photocatalytic efficiency. *Journal of the American Chemical Society*, 133(41): 16414-16417.

